

**THREE-DIMENSIONAL MORPHOLOGY OF THE ICHNOFOSSIL
PHYCOSIPHON INCERTUM AND ITS IMPLICATION FOR
PALEOSLOPE INCLINATION**

HAJIME NARUSE* AND KO NIFUKU

Division of Earth and Planetary Sciences, Graduate School of Science, Kyoto University,

Kitashirakawa Oiwakecho, Sakyo-ku, Kyoto 606-8502, Japan

e-mail: naruse@kueps.kyoto-u.ac.jp

*Corresponding author

*Current address: Department of Earth Sciences, Faculty of Science, Chiba University,
1-33 Yayoicho, Inage-ku, Chiba 263-8522, Japan; E-mail: naruse@faculty.chiba-u.jp

*RRH: MORPHOLOGY OF PHYCOSIPHON INCERTUM AND IMPLICATION FOR
PALEOSLOPE INCLINATION*

LRH: NARUSE AND NIFUKU

Key words: Trace fossil, Sediment compaction, Slump scar, Submarine slope,
Three-dimensional visualization

ABSTRACT

Details of the three-dimensional morphology of the ichnofossil *Phycosiphon incertum* collected from deposits on submarine slopes are reconstructed by processing a series of images obtained from polished sections of the samples. Samples were collected from the mudstone around a slump scar in the Paleocene Shiomi Formation, Northern Japan, which is characterized by the occurrence of slump scars. The reconstructed morphology of *Phycosiphon incertum* is a meandering tube with a flattened ellipse cross section. The tubes are flattened in a plane oblique to the bedding surfaces, and aligned along the same direction at both the interior and exterior of the slump scar. Flattening of the tubes was caused likely by sediment compaction, and the tube flattens toward the horizontal plane that is oblique to the bedding plane because of the paleoslope inclination. The difference between the bedding and flattening planes of the tubes of *Phycosiphon incertum* may imply paleoslope inclination. When the inclination of the bedding plane of the Shiomi Formation is corrected using the flattened surfaces, the bedding plane dips by 9° toward the southeast, which conforms to the paleocurrent direction of the turbidites. The morphology of *Phycosiphon incertum* can, therefore, be used as a paleoslope indicator.

INTRODUCTION

In this study we introduce an unusual mode of *Phycosiphon incertum* occurrence in the deposit of a submarine slope. The ichnogenus *Phycosiphon incertum* von Fischer–Ooster, 1858, is an ichnofossil composed of narrow and sinuous tubes that irregularly twist, and

they comprise a series of closely packed loops with a poorly defined pale mantle (Kern, 1978; Goldring et al., 1991; Wetzel and Bromley, 1994; Fig. 1). The tube diameter is normally less than 1 mm and the lobes have widths ranging from several millimeters to approximately 1 cm. In sections, *Phycosiphon* resembles clusters of closely spaced spots or comma-shaped dots and hooks filled with darker and finer sediments surrounded by narrow (~1 mm) pale mantles. Generally, various orientations of the lobes result in a chaotic arrangement of dark cores in the sections. This ichnofossil is characterized by the presence of a spreite-containing material that is not as fine as the surrounding sediment and trace meniscus backfilled tubes (e.g., Seilacher, 1962; Wetzel and Bromley, 1994); the preservation of the spreite, however, is typically quite poor (Fu, 1991).

Studies suggest that an opportunistic deposit feeder produced *Phycosiphon* (Goldring et al., 1991; Wetzel and Bromley, 1994; Wetzel and Uchman, 2001). *Phycosiphon* is found in muddy siltstone and sandstone in Paleozoic to Holocene strata deposited in broad range of environments from continental shelves to submarine fans (Goldring et al., 1991; Fu, 1991; Savdra et al., 2001). Crosscutting relationships of the ichnofossils suggests that the *Phycosiphon* producers are probably the first organisms colonizing the upper part of a turbidite (5–40 mm below the seafloor) in a very short time after deposition (Wetzel and Uchman, 2001).

Usually, the burrow cores of *Phycosiphon* are variably oriented or lie parallel to bedding planes (Bromley, 1996); however, we observed *Phycosiphon* inclined uniformly to the bedding plane (Fig. 1). This research suggests that *Phycosiphon incertum* is closely related to ancient slope inclination and, therefore, may be an indicator of paleoslope.

In order understand better the morphology of *Phycosiphon incertum*, a three-dimensional

visualization technique was developed using sequential images of polished sections of an ichnofossil sample. Serial polishing is a common method to observe trace fossils (Uchman, 1995; Wetzel and Uchman, 2001); however, visualization using computer graphics enables a quantitative examination of their morphologic features (e.g., Gingras et al., 2002).

Phycosiphon incertum is one of the smallest ichnofossils with complex morphological features; therefore, visualization would confirm the effectiveness of our method for application to ichnofossil morphology research.

GEOLOGIC SETTINGS

The study area is situated on the Pacific Coast of the eastern part of Hokkaido Island, which is at the western end of the Kuril Arc (Fig. 2). The Kuril Arc is a subduction zone that extends from Hokkaido Island in northern Japan to the Kamchatka Peninsula in eastern Russia. In the southwestern Kuril Arc, the volcanic islands are arranged *en echelon*, and the frontal arc is traced from the Nemuro Peninsula in Hokkaido to the middle part of the Kuril arc. It is inferred that the southwestern end of this arc has been colliding with the Tohoku Arc of Japan since the Miocene, thereby raising the Hidaka Mountains of Hokkaido Island (Kimura, 1986).

Samples of *Phycosiphon incertum* studied were collected from the Shiomi Formation, located in the upper part of the Cretaceous-Paleocene Nemuro Group in eastern Hokkaido (Fig. 2). The Nemuro Group was deposited in the fore-arc basin of the Kuril Arc (Kiminami, 1983; Naruse, 2003); the upper part characterized by numerous slump scars that possess concave-upward semicircular erosional surfaces with diameters of hundreds of meters (Naruse, 2003). Slump scars are characteristic of ancient subaqueous slumping (Clari and

Ghibaudo, 1979), therefore, the upper part of the group was likely deposited on a submarine slope (Naruse, 2003).

The Shiomi Formation overlies the Senposhi Formation (although the boundary separating the two is not exposed) and is overlain unconformably by the Kombumori Formation, all of which are in the upper part of the Nemuro Group (Fig. 3; Sassa et al., 1952). Shiomi Formation is more than 440 m thick and consists mainly of bioturbated sandy siltstone, lenticular-bedded conglomerate (<1 m thick), and alternating thinly bedded (mostly <30 cm thick) fine-grained sandstone and mudstone. Most sedimentary rocks in the formation contain volcanoclastics (Kiminami, 1979), and the formation is partially intruded by basaltic dikes. In the study area, the bedding strikes along the east–west direction and dips 6°–20° to the south (Fig. 2C). Distinct tectonic folding is not observed. Such fossils as *Terebratulina* sp. and *Acila hokkaidoensis* are observed in this formation, suggesting a shelf-edge to slope environments (Kawai, 1956).

SLUMP SCARS IN THE SHIOMI FORMATION

The Shiomi Formation outcrop is about 12 m in height and extends continuously for 1 km from east to west (Fig. 4), almost parallel to the strike of the strata (Fig. 2C). The strata exposed in the outcrop are generally composed of alternating beds of bioturbated sandy siltstone and thin-bedded turbiditic sandstone (Fig. 5), which dip 10° southward. Lenticular-bedded conglomerates are also present in this outcrop. Two intraformational discordances, both of which dip westward, are observed at the eastern end of the outcrop, in which the upper discordance truncates the lower one (Fig. 4–5). On the other hand, another set of discordances are at a location ~270 m west from the eastern discordances. The

western surfaces of the discordances gently dip eastward, and the upper surface also truncates the lower surface (Fig. 4). All surfaces of the discordances are smooth, gently concave upward, and show no features that suggest minor erosional scouring.

All the discordances truncate the intensely bioturbated sandy siltstone intercalated with the thin-bedded turbidites, and the sedimentary fills on the discordances are identical to the truncated lower sediments (Fig. 5B). Beds overlying the discordances exhibit a characteristic upward flattening of the bed surfaces, which in the lower part partially overlap or drape the surface of the discordance (Fig. 4). Turbidite bedding planes above the discordance are oblique by $\sim 20^\circ$ to those below the surface of the discordance because the beds drape the discordance inclined westward at the eastern end of the outcrop. The paleocurrent direction of the turbidites both above and below the surfaces of the discordances is from NW to SE (Fig. 6).

These erosional features probably represent the slump scars left behind by the periodic downslope sliding of the strata packets (Clari and Ghibaudo, 1979). Considering the locations and concave-upward features of the sedimentary fills, the eastern and western sets of the erosional surfaces in the outcrop are likely connected and comprise two concave-upward, semicircular erosional surfaces intersecting each other. The lateral extent of the individual discordances cannot be determined due to the truncation by subsequent discordances and limited outcrop; however, the concave-upward submarine escarpments were likely more than 270 m wide and 10–30 m deep (Fig. 4).

Clari and Ghibaudo (1979) described numerous concave-upward discordances as slump scars in the shelf edge to the upper submarine slope facies of the Miocene sequence. They proposed criteria to distinguish slump scars in strata: (1) absence of erosional scouring or

channel lag, (2) sedimentary fills in the discordance virtually identical to surrounding sediments, and (3) sedimentary fills show characteristic upward flattening of bed surfaces. All these features are applicable to the discordances in the outcrop of the Shiomi Formation, and the intersection of the erosional surfaces is also a common feature of the slump scars (Clari and Ghibauod, 1979). Due to the fine-grained sedimentary fills and the absence of minor scouring features, these semicircular erosional surfaces are not likely submarine channels, which are usually filled by coarser materials and often have irregular scouring features at their bases (Naruse, 2003). The concave-upward slump scars are a common topographic feature in the upper part of the submarine slopes (e.g., Aksu and Hiscott, 1992). van Weering et al. (1998) reported slump scars with a width of 100–500 m in their seismic and side-scan sonar images of a modern submarine slope at the North-East Faeroe continental margin. Those escarpment sizes match the scale of the discordances found in the Shiomi Formation.

VISUAL REPRESENTATION OF *PHYCOSIPHON INCERTUM*

Phycosiphon incertum occurs preferentially in coarse siltstone and fine-grained sandstone at the outcrop of the Shiomi Formation that exhibits the erosional surfaces of the slump scars. The ichnofossil shows a condensed distribution of patches with a diameter or height of 3–10 cm thick in coarse siltstone above the turbidites.

Phycosiphon incertum is a small but complex burrow comprising a dark core with a light mantle when viewed in cross section (Fig. 1, 7). In outcrop or in polished section, the dark-colored burrow core appears in the form of elliptical spots, lengths, or hooks 0.5 mm thick, which consist of finer sediments with hints of meniscus backfill (Fig. 7B). In vertical

section, the core spots elongate obliquely with respect to the bedding plane (Fig. 1, 7A). The angle between the elongation direction of the core spots and the bedding planes tends to be larger in the interior of the slump scars than in the exterior. U-shaped hooks of the burrow cores are oriented along various directions in the polished sections, exhibiting tight loops of tubes that deviate from the horizontal plane. The mantle of the burrow is white in color and composed of materials coarser than that in the burrow cores and surrounding sediments. Spreite is occasionally observed in the mantle (Fig. 7C). The width of the mantle is 2–3 times larger than the diameter of the core (Fig. 7A), although it is usually difficult to distinguish a discrete mantle because the burrows are generally concentrated in the sediments.

All the features of the ichnofossil described here are similar to previous descriptions of *Phycosiphon incertum* (Goldring et al., 1991; Wetzel and Bromley, 1994); however, the alignment of the burrow-core spots uniformly oblique to the bedding plane is an unusual characteristic of this ichnogenera. Although the morphology of *Phycosiphon incertum* varies in different rock types, the lobes normally lie nearly horizontal or parallel to the lamination in the vertical sections (Wetzel and Bromley, 1994).

MEASUREMENTS OF *PHYCOSIPHON INCERTUM* ON THE POLISHED SECTIONS

The size distribution, aspect ratio (length/width), and apparent orientations of the dark-colored burrow cores observed in the sections were measured by using the image analysis software ImageJ (<http://rsb.info.nih.gov/ij/>). Each dark core in the vertical cross-sectional image was automatically approximated by an ellipse. Here, the length of the

long and short axes, the aspect ratio (long-axis/short-axis), and long-axis orientation of the approximated ellipse are defined as the size, aspect ratio, and orientation of the burrow core, respectively. All direction measurements are based on the magnetic coordination.

Size distribution and aspect ratio.—The modal sizes of the long and short axes of burrow cores are 1.35 and 0.38 mm, respectively, and both their size distributions have long tails toward the larger size (Fig. 8), because spot-shaped and hook-shaped cores were measured. As a result, the modal value of the aspect ratio of the dark-colored cores is approximately 3–4 with the long-tailed distribution (Fig. 8). The size distribution and aspect ratio of the cores for the samples collected from the interior and exterior of the slump scars do not exhibit significant differences.

The orientation in the vertical section.—All burrow cores are oriented along the same direction, namely, oblique to the bedding plane, both in the interior and exterior of the slump scars (Fig. 9). At the interior of the slump scars, the burrow cores are inclined 6.16° westward and 5.12° southward on the vector average in the E–W and N–S vertical sections with 1.10° and 1.02° of the 95% significant interval, respectively (Fig. 9A–B). At the exterior of the slump scars, their inclination averages 8.07° westward and 3.64° southward in the E–W and N–S vertical sections with 1.63° and 1.45° of the 95% significant interval, respectively (Fig. 9C–D). In summary, their preferred orientation matches both in the interior and the exterior within significant intervals. The inclination of the core spots to the bedding surfaces, however, tend to be larger at the interior of the slump scars than at the exterior because the inclination of the bedding surfaces differs in both the horizons due to slumping. It is oblique by 9° at the exterior of the slump scar and by 18.8° at the interior of the slump scar (Fig. 10A–B).

THREE-DIMENSIONAL MORPHOLOGY OF *PHYCOSIPHON INCERTUM*

The three-dimensional morphology of *Phycosiphon incertum* in sandy siltstones of the Shiomi Formation was visualized by using computer graphics. The oriented specimen was collected from the interior of the slump scars in outcrop, and it was then polished and photographed in order to acquire sequential section images with constant displacement. The series of acquired images was processed to visualize the morphology of the ichnofossil (Fig. 11).

Methodology

1) *Sample preparation and image acquisition.*—Sequential gray-scale images of the sections were acquired by polishing the oriented sample repeatedly with constant displacement (Fig. 11A). Each polished section was digitally photographed by using a flatbed image scanner with a resolution of 47.2 pixels per mm (1200 dpi). The polishing plane in the sample should be chosen so as to optimize the resolution to the property of the research objective. This is necessary because the resulting three-dimensional data generally has the maximum resolution along the axes parallel to the polished sections (X and Z axes) and the minimum resolution along the axis normal to the sections (Y-axis), where the spacing between each section defines the resolution on the Y-axis. In the case of *Phycosiphon*, the burrow cross section cores appear to be ellipses that orient their shortest axes nearly vertical so that the Y-axis cannot be assigned to the vertical direction. The E–W-oriented vertical sections, therefore, were selected as the planes along which the specimen sections were to be polished. Also, the Y-axis in the coordinate system of the resulting three-dimensional data was assigned to the N–S horizontal direction. Since the

smallest size of the burrow cores is around 0.5 mm, the spacing of the section images was set to 0.5 mm in this study.

2) *Image preprocessing and classification.*—The acquired images were processed to select the regions to observe in the three-dimensional image (Fig. 11B–D). First, as a preprocessing step, image filtering (median filter) was applied to the acquired sequential images to reduce the random electronic noise introduced during image acquisition. Image classification was then performed by dividing the image into regions corresponding to the burrow cores and the other regions including the mantle of *Phycosiphon* using the *k*-means clustering classification scheme (Russ, 2002), which is a brightness-based pixel classification procedure. Due to good contrast between the cores and other regions in the images, the threshold brightness was determined automatically. The classified images were then converted into binary images in which white pixels represented the cores of *Phycosiphon incertum* and black pixels represented other regions.

3) *Image post-processing.*—Because the sample contains too many cores to examine the discrete morphology of the burrow, three continuous burrows were manually selected as objectives to observe in this study, and the other cores were erased from the images (Fig. 11E). Finally, the resolution of each image was reduced for decreasing the difference in the resolution between the axes parallel and normal to the section plane. Without this final procedure of image postprocessing, the structures along the polished sections would be overemphasized in the rendered three-dimensional image. The resolution of the images was reduced to 10 pixels per mm, which is still 5 times as fine as that along the Y-axis.

4) *Three-dimensional volume rendering*— The burrow surface was visualized from the three-dimensional volume data (Fig. 11F). The binary sequential images were converted

into a three-dimensional array by the software, and the surfaces of the burrow cores were computed by connecting the boundary points between the black and white pixels. Computation was performed by using the commercial software MATLAB 6.5.1 (MathWorks Inc., 2003).

Result

The reconstructed morphology of *Phycosiphon incertum* in the computer graphic image was a tightly meandering tube whose cross section was a flattened ellipse (Fig. 12). Although the burrow itself meanders in various three-dimensional directions, the range of burrows penetrating the sediment appears to be restricted by the horizons parallel to the bedding planes (Fig. 12C), which are about 5 mm thick.

In contrast, the directions of the flattened burrows follow a plane oblique to the bedding surfaces of the strata (Fig. 12D). All the flattening planes are oriented along the same direction, and their inclination to the bedding surfaces is approximately 20°, concordant with the estimation from measurements of the polished sections (Fig. 9, 12D).

The shape of the meandering lobes in *Phycosiphon* tubes varies depending on their angle against the flattening plane of the burrow cross section (Fig. 12B). The lobes perpendicular to the flattening planes are remarkably tight in comparison with those parallel to the flattening planes. In addition, the burrows thicken and their cross section is rounded at the bend of the loops perpendicular to the flattening plane (Fig. 12–13).

DISCUSSION

Reconstructed Morphology of *Phycosiphon incertum*

Three-dimensional features of *Phycosiphon incertum* in the Shiomi Formation are first visualized by the image analysis technique presented here. Although serial polishing has been used as a common method for observing trace fossils (Uchman, 1995; Wetzel and Uchman, 2001), visualization computer graphics enables more detailed observation and quantitative measurements. Wetzel and Bromley (1994) reported the three-dimensional morphology of *Phycosiphon* by means of the X-ray radiograph obtained from the Holocene sediments of the Sulu Sea (Wetzel and Bromley, 1994, fig. 4); however, they also suggested that the sample of the ancient trace fossils had a similar X-ray density to the matrix and showed a poor contrast because of diagenesis. Visualization by using X-ray computed tomography appears to be unavailable for a similar reason. The image analysis of sequential section images, therefore, is probably the best method of examining three-dimensional features of the ichnofossil preserved in the strata.

Our method successfully reconstructed the three-dimensional morphology of *Phycosiphon incertum*; it is a tightly looped tube with a flattened elliptic cross section. *Phycosiphon incertum* was defined as a small trace fossil consisting of a tube recurving as a series of lobes (Fischer-Ooster, 1858). Wetzel and Bromley (1994) showed that *Phycosiphon* is an extensive small-scale spreite trace fossil comprising repeated narrow, U-shaped lobes that enclosed a spreite with dimensions of the order of mms to cms, and branching regularly or irregularly from an axial spreite of similar width (Wetzel and Bromley, 1994, fig. 4). The characteristics of *Phycosiphon* as tightly meandering lobes,

vertical and horizontal lobes co-occurring within one system, and thickening of tubes near the apex of the spreite (Wetzel and Bromley, 1994) are clearly represented in the computer graphic image (Fig. 12); only the branching is not shown. This suggests the effectiveness of our visualization method.

Although the tube itself meanders in various three-dimensional directions, a range of tubes penetrating the sediments appears to be restricted by the horizons parallel to the bedding planes (Fig. 12E). This burrowing range might be a reflection of the restriction related to the habitat of producers, such as the oxygen concentration or the amount of nutrition in the sediments.

The difference between the X-ray radiograph of Holocene sediments and the reconstruction in this study is that the flattened shape of the burrow tubes and the variation in the lobe morphology depends on the direction of the lobe (Wetzel and Bromley, 1994, fig. 4). In our opinion, the different features of *Phycosiphon incertum* observed can be attributed to sediment compaction. The influences of sediment compaction are discussed in the next section.

Influence of Sediment Compaction

Our interpretation is that the flattened elliptic cross section of *Phycosiphon incertum* can be attributed to the compaction of sediments. Meniscus backfilling in the burrow cores suggests that the burrow cross section must originally reflect the body shape of the tracemaker; further, it is unlikely that the elliptic shape of the burrow is the original morphology of the tracemaker since the cross sections of the tubes appear to be rounded at the section parallel to the flattening plane (Fig. 13). The fact that the orientation of the

flattening planes of burrows is invariant irrespective of paleotopographic change, e.g., slump scars, implies that the flattening plane corresponds to the gravitationally horizontal plane in the original configuration of the strata.

The variation in the curvature and thickness of the loops of burrow tubes can also be explained by the influence of sediment compaction (Fig. 12). The compaction shortens the distance between two vertical burrow tubes; this causes an apparent tightening at the apex of loops having a perpendicular orientation to the flattening plane and a relative loosening for a parallel orientation. Further, a relative thickening of tubes at the apex of the vertical loops actually exhibits a thinning of the horizontal tubes. In this manner, we conclude that the morphology of the ichnofossil was flattened by the sediment compaction probably due to the dewatering of unconsolidated sediments.

If we assume that the elliptic cross section of cores is a result of the shrinkage of muddy sediments, the initial porosity ϕ_o of sediments where the *Phycosiphon* producers dwelled can be roughly estimated from the aspect ratio of burrow cores. Typically, the compaction of muddy sediments causes an exponential decrease in the sediment porosity as follows (Magara, 1978):

$$\phi = \phi_o e^{-cz} \quad (1)$$

where ϕ is porosity of sediments, z is depth of burial, and c is an empirical coefficient of compaction (approximately $1.42 \times 10^{-3} \text{ m}^{-1}$) (Magara, 1978). The porosity of the initial sediment can, therefore, be calculated from the following equation:

$$\phi_o = \frac{a-1}{a(1-e^{-cz})} \quad (2)$$

where a is an aspect ratio of long /short axes of tube cross sections. The measurements for the vertical sections indicated that the aspect ratio of burrow cores is 3.55 in mode (Fig. 8), which means the rate of sediment shrinkage is approximately 28%. Although the aspect ratio of the burrow cores in the vertical polished sections are not exactly equal to that in the burrow cross sections except for the case that the flattening plane is completely horizontal, we assume that our measurements in the vertical sections are not significantly different because the inclination of the flattening plane is only 8° . Then, we roughly estimate the burial depth z to be more than 1500 m by adding the thickness of the overlying Kombumori Formation and the Urahoro Group (Nanayama et al., 1994). The Shiomi Formation obviously experienced considerably deeper burial because the overlying Urahoro Group is also composed of consolidated sedimentary rocks; however, even if the burial is at a depth greater than 5000 m, there is no change in the sediment porosity. Thus, when we tentatively estimate the range of burial depth z from 1500 to 5000 m, the initial porosity ϕ_o ranges from 72–82%; this is analogous to that of the modern argillaceous sediments whose porosities of 77–87% occur in the top 3 m of the sediment (Raiswell, 1976). Our estimation, therefore, suggests that sediment compaction can easily lead to the deformation of the ichnofossils observed in this study.

The morphology of *Phycosiphon* can be retrodeformed if the burrows were originally rounded and were deformed by pure shear strain due to the compaction of the sediment layer. If it is assumed that they strained only along the direction normal to the flattening plane, we obtain the strain tensor \mathbf{F} as follows:

$$\mathbf{F} = \mathbf{Q} \begin{pmatrix} 1 & 0 & 0 \\ 0 & 1 & 0 \\ 0 & 0 & 1/a \end{pmatrix} \mathbf{Q}^T \quad (3)$$

where

$$\mathbf{Q} = \begin{pmatrix} \cos \varphi & -\sin \varphi \cos \theta & -\sin \varphi \sin \theta \\ \sin \varphi & -\sin \varphi \cos \theta & \cos \varphi \sin \theta \\ 0 & -\sin \theta & \cos \theta \end{pmatrix} \quad (4)$$

and φ and θ are the dip direction and dip of the flattening plane of the burrows, respectively. Figure 14 shows the result of the retrodeformation of *Phycosiphon* by using \mathbf{F}^{-1} that is calculated from the values $a = 3.55$, $\varphi = -122^\circ$, and $\theta = 8.3^\circ$.

Retrodeformed burrow tubes exhibit isotropic features such as a constantly rounded shape of tubes and similar curvatures at the apex of both vertical and horizontal lobes (Fig. 14). Moreover, the reasonable result of retrodeformation confirms our inference that several features of *Phycosiphon incertum* were a result of the sediment compaction.

We infer that the extensively flattened geometry of *Phycosiphon* can be attributed to the opportunistic habitat of its producers. It has been suggested that *Phycosiphon incertum* is generally affected by intense compaction (Goldring et al., 1991; Wetzel and Bromley, 1994), and an examination of the crosscutting relationships of the ichnofossils suggests that the producers of *Phycosiphon* enter well-oxygenated muds at 5–40 mm below the sediment surface prior to other producers of the co-occurring ichnofossils (Wetzel and Uchman, 2001). *Phycosiphon* was likely the first burrows produced in unconsolidated mud-bearing abundant interstitial water, and hence, it appears to be the most capable of being compacted among the co-occurring ichnofabrics. In fact, *Chondrites*, which penetrates sediments late

and deep, appears to be less deformed in comparison with the flattened geometry of co-occurring *Phycosiphon* (Goldring, 1991, figs. 5A and 9; Wetzel and Uchman, 2001, fig. 5). The geometry of *Phycosiphon*, thus appears to be sensitive to the dewatering of sediments, and it can be a good strain marker of the initial sediment compaction.

Paleoslope Inclination Suggested by the Geometry of *Phycosiphon incertum*

Although the occurrence of slump scars clearly implies that the Shiomi Formation was deposited on a submarine slope (Fig. 4), it is generally difficult to identify submarine slopes from ancient deposits because the tectonic movement after deposition tilts the inclination of the bedding planes in strata. Thus, in order to examine the topographic features of ancient submarine slopes, a tilting correction of bedding planes is necessary on the basis of a marker of the original horizontal plane in strata.

We suggest a possibility that the geometry of *Phycosiphon incertum* is available as a marker of the original horizontal plane in strata. Our results suggest that *Phycosiphon* shows deformation by sediment compaction in a relatively short period after its burial, implying that its flattening plane probably corresponds to the gravitationally horizontal plane during the deposition of strata. In fact, its flattening plane is invariable both in the interior and exterior of slump scars, and its higher inclination to the bedding plane in the interior of scars can be interpreted to result from the high topographic inclination of submarine escarpments.

For instance, if the bedding plane at the exterior of slump scars in the Shiomi Formation (dip-direction and dip are N171°E and 10°) is rotated using the flattening plane of *Phycosiphon* (dip-direction and dip are N130°W and 8°) as a marker of the horizontal plane,

the corrected bedding plane dips toward southeast (N122°E) with 9° inclination (Fig. 15). The reconstructed dip direction of the submarine slope is conformable to the paleocurrent direction of turbidites in the Shiomi Formation (Fig. 15).

The 9° gradient of the submarine slope in the Shiomi Formation appears reasonable. Gradients of the submarine slope range from 3–6° or less on mud-dominated, passive-margin slopes (Heezen et al., 1959), to 10–30° on erosional slopes flanking such strike-slip basins as those found along the North Anatolian Transform Fault of northwestern Turkey (Aksu et al., 2000). In cases where a high sediment yield results in a line-source input to the submarine slope, such as in tectonically active regions or seaward of modern continental shelves formerly covered by Quaternary continental ice sheets, submarine slopes tend to dip 6–10 degrees (e.g., Hiscott and Aksu 1994). The Shiomi Formation is supposed to have been deposited on the tectonically active region (Kiminami, 1983; Naruse, 2003), and, therefore, it is possible that the formation deposited on the slope dips approximately 9° south-eastward.

Judging from the results for the Shiomi Formation, we propose that the flattening plane of *Phycosiphon* is probably a marker of topographic reconstruction, especially in the tectonically active region where slope gradients are relatively high, even though further verifications are necessary in future studies. All ichnofossils that have rounded tubes appear to be useful for the identification of the horizontal plane in strata; however, *Phycosiphon* is probably the most suitable for geomorphologic analysis because of their geometric sensitivity for the sediment compaction.

CONCLUSIONS

The three-dimensional morphology of the ichnofossil *Phycosiphon incertum* was reconstructed from a series of polished section images by using computer graphics. The conclusions are as follows:

(1) The reconstructed geometry of *Phycosiphon incertum* is a meandering tube that is quite similar in morphology to that observed in the X-ray radiograph recorded from Holocene sediments. Thus, the visualization method presented here is useful to examine the morphology of the ichnofossils preserved in ancient deposits.

(2) The geometry of *Phycosiphon* was strongly affected by sediment compaction. The cross section of the reconstructed burrow was elliptical, which is a deformation from the initially circular cross section.

(3) The difference between the bedding and flattening planes of the tubes of *Phycosiphon incertum* might imply paleoslope inclination. For instance, when we corrected the inclination of the bedding plane of the Shiomi Formation by using the flattening surface measured, we observed that the bedding plane dips by 9° toward the southeast, which conforms to the paleocurrent direction of the turbidites. There, therefore, is a possibility that the three-dimensional morphology of *Phycosiphon incertum* can be a paleoslope indicator.

ACKNOWLEDGEMENTS

We thank Dr. R. Steel for his constructive comments, and are grateful to Drs. T. Ubukata and M. Nara for helpful discussion and advice. This manuscript benefited from thoughtful reviews by two anonymous reviewers. Gratitude is extended to Editor Stephen T. Hasiotis

and Associate Editor. This research was funded in part by a Grant-in-Aid for Young Scientists (B) (16740287, 2004) from the Ministry of Education, Science, Sports, Culture and Technology of Japan.

REFERENCES

- AKSU, A.E. and HISCOTT, R.N., 1992, Shingled Quaternary debris flow lenses on the North-east Newfoundland Slope: *Sedimentology*, v. 39, p. 193-206.
- AKSU, A.E, CALON, T.J.; AND HISCOTT, R.N, 2000, Anatomy of the North Anatolian fault zone in the Marmara Sea, western Turkey; extensional basins above a continental transform: *GSA Today*, v. 10, p. 3-7.
- BROMLEY, R.G., 1996, Trace fossils; biology, taphonomy and applications: Chapman & Hall, London, United Kingdom, 840 p.
- CLARI, P. and GHIBAUDO, G., 1979, Multiple slump scars in the Tortonian type area (Piedmont Basin, northwestern Italy): *Sedimentology*, v. 26, p. 719-730.
- FISCHER-OOSTER, C.VON., 1858, Die fossilen Fucoiden der Schweizer Alpen, nebst Erörterung über deren geologisches Alter. Huber und Companie, Berlin, 74 p.
- FU, S., 1991, Funktion, Verhalten, und Einteilung fucoider und lophocteniider Lebensspuren: E. Schweizerbart'sche Verlagsbuchhandlung, Stuttgart, 79 p.
- GINGRAS, M.K, MACMILLAN, B., BALCOM, B.J., SAUNDERS, T., AND PEMBERTON, S.G., 2002 Using magnetic resonance imaging and petrographic techniques to understand the textural attributes and porosity distribution in *Macaronichnus*-burrowed sandstone: *Journal of Sedimentary Research*, v. 72, p. 552-558.
- GOLDRING, R., POLLARD, J.E., AND TAYLOR, A.M., 1991, *Anconichnus horizontalis*; a

- pervasive ichnofabric-forming trace fossil in post-Paleozoic offshore siliciclastic facies: *Palaios*, v. 6, p. 250-263.
- HEEZEN, B.C., THARP, M., AND EWING, W.M., 1959, The North Atlantic; text to accompany the Physiographic diagram of the North Atlantic, [Part] 1 of The floors of the oceans: Geological Society of America, Boulder, 122 p.
- HISCOTT, R.N., AND AKSU, A.E., 1994, Submarine debris flows and continental slope evolution in front of Quaternary ice sheets, Baffin Bay, Canadian Arctic: *AAPG Bulletin*, v. 78, p. 445-460.
- KAWAI, M., 1956, Explanatory text of the geological map of Japan, scale 1:50,000; kombumori (Kushiro-48): Geological Survey of Japan, Tsukuba, 8 p.
- KERN, J.P., 1978, Paleoenvironment of new trace fossils from the Eocene Mission Valley Formation, California: *Journal of Paleontology*, v. 52, p. 186-194.
- KIMINAMI, K., 1979. Sedimentary petrography of the Nemuro Group: *Chikyū Kagaku*, v. 33, p. 152–162.
- KIMINAMI, K., 1983, Sedimentary history of the Late Cretaceous–Paleocene Nemuro Group, Hokkaido, Japan: a forearc basin of the Paleo-Kuril arc-trench system: *Journal of Geological Society of Japan*, v. 89, p. 607–624.
- KIMURA, G., 1986. Oblique subduction and collision: forearc tectonics of the Kuril arc: *Geology*, v. 14, p. 404-407.
- MAGARA, K., 1978, *Compaction and fluid migration; practical petroleum geology*: Elsevier, Amsterdam, 319 p.
- MATHWORKS INC., 2003, *MATLAB 6.5.1 [CD-ROM]*: Natick, Commonwealth of Massachusetts, USA.

- NANAYAMA, F., NAKAGAWA, M., AND KATOH, T., 1993, Chemistry of detrital chromian spinel in Latest Cretaceous to Paleocene sediments from eastern Hokkaido: *Chishitsugaku Zassh*, v. 98, p. 1041-1059.
- NARUSE, H., 2003, Cretaceous to Paleocene depositional history of North-Pacific subduction zone; reconstruction from the Nemuro Group, eastern Hokkaido, northern Japan: *Cretaceous Research*, v. 24, p. 55-71.
- RAISWELL, R., 1976, The microbiological formation of carbonate concretions in the Upper Lias of N.E. England: *Chemical Geology*, v. 18, p. 227-244.
- RUSS, J.C., 2002, *The Image Processing Handbook, Fourth Edition*: CRC Press, Boca Ration, Florida, 732 p.
- SAVDRA, C.E., KRAWINKEL, H., MCCARTHY, F.M.G., MCHUGH, C.M.G., OLSON, H.C., AND MOUNTAIN, G., 2001, Ichnofabrics of a Pleistocene slope succession, New Jersey margin: relations to climate and sea-level dynamics: *Palaeogeography, Palaeoclimatology, Palaeoecology*, v. 171, p. 41-61.
- UCHMAN, A., 1995, Tiering patterns of trace fossils in the Palaeogene Flysch deposits of the Carpathians Poland: *Geobios Special Memoir*, v. 18, p. 389-394.
- VAN WEERING, T.C.E., NIELSEN, T., KENYON, N.H., AKENTIEVA, K., KUIJPERS, A.H., 1998, Sediments and sedimentation at the NE Faeroe continental margin; contourites and large-scale sliding: *Marine Geology*, v. 152, p. 159-176.
- WETZEL, A., AND BROMLEY, R.G., 1994, *Phycosiphon incertum* revisited: *Anconichnus horizontalis* is junior subjective synonym: *Journal of Paleontology*, v. 68, p. 1396-1402.

WETZEL, A, UCHMAN, A., 2001, Sequential colonization of muddy turbidites in the Eocene Belovežľa Formation, Carpathians, Poland: *Palaeogeography, Paleoclimatology, Palaeoecology*, v. 168, p. 178-202.

FIGURE 1—Vertical section of the ichnofossil *Phycosiphon incertum* in sandy siltstone. The lower part of the section is the bedding surface of the turbidite and the ichnofossils are uniformly oblique with respect to the bedding plane suggested by a dashed line. Scale is 1 cm.

FIGURE 2—Distribution of the Nemuro Group and location of the study area. Modified based on Kusunoki and Kimura (1998). A) Arc–arc junctions around the Japanese islands. B) Distribution of the Nemuro and Urahoro groups and location of the study area. C) Geological map of the study-areas; for locations.

FIGURE 3—Lithostratigraphic subdivision of the Nemuro and Urahoro groups in the study area.

FIGURE 4—Mosaic photograph and sketch of the slump scars in the Shiomi Formation. Black arrows indicate the location of the discordances. Strikes and dips of the bedding surfaces change gradually because of the concave-upward topography of the slump scars.

FIGURE 5—A) Field photograph of the sampling points. Samples were collected at the interior (a) and exterior (b) of the slump scars. Scale is 5 m. B) Lithologic columnar sections at the outcrop studied.

FIGURE 6—Rose diagram suggesting that the paleocurrent direction of the turbidites in the Shiomi Formation is generally oriented southeastward.

FIGURE 7—Visual description of *Phycosiphon incertum* in vertical sections. A) Vertical section of *Phycosiphon incertum* that is oblique to the bedding plane. The black arrow indicates the core and the white arrow indicates the mantle of the burrows. Scale is 1 cm. B) Meniscus backfilling in the core of *Phycosiphon incertum* indicated by white arrows. Scale is 2 mm. C) Spreite in the mantle of the burrow indicated by white arrows. Scale is 1

mm.

FIGURE 8—Size distribution of the cores of *Phycosiphon incertum* in the vertical section. A) Summarized data collected from all locations. B) Measurement along the E–W-oriented vertical section obtained from the interior of the slump scars. C) Measurement along the E–W-oriented vertical sections obtained from the exterior of the slump scars. D) Measurement along the N–S-oriented vertical sections obtained from the interior of the slump scars. E) Measurement along the N–S-oriented vertical sections obtained from the exterior of the slump scars.

FIGURE 9—Rose diagrams showing the apparent orientations of the burrow cores in the vertical sections. A) Orientation in E–W-oriented vertical sections obtained from the interior of the slump scars. B) Orientation in E–W-oriented vertical sections obtained from the exterior of the slump scars. C) Orientation in N–S-oriented vertical sections obtained from the interior of the slump scars. D) Orientation in N–S-oriented vertical sections obtained from the exterior of the slump scars.

FIGURE 10—A) Stereonet diagram showing bedding and orientation planes of *Phycosiphon incertum* in both the interior and exterior of slump scars. B) Schematic diagram of the relationship between the *Phycosiphon* orientation and bedding planes.

FIGURE 11—Procedures of three-dimensional visualization of *Phycosiphon*. A) Sequential gray-scale images of the sections acquired by polishing the oriented sample repeatedly with a constant displacement. B) Each polished section was digitally photographed by using a flat-bed image scanner. C) Image filtering (median filter) was applied to the acquired sequential images to reduce random electronic noise introduced during image acquisition. D) Image classification was then performed by dividing the image

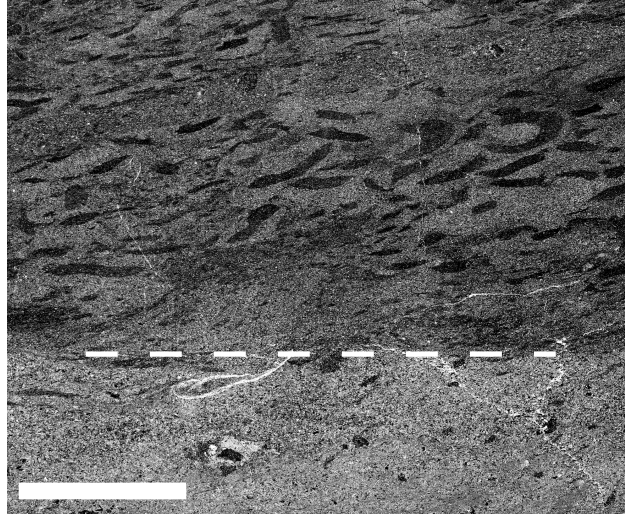
into regions corresponding to burrow cores and other regions including the mantle of *Phycosiphon* using the *k*-means clustering classification scheme. E) Continuous burrow tubes were manually selected as objectives to observe, erasing other cores in the images. F) The surface of the ichnofossil was visualized from the three-dimensional volume data.

FIGURE 12—Rendered images of *Phycosiphon incertum*. A) Morphology of *Phycosiphon incertum* from the viewpoint of the direction toward northwest. Vertical lobe (a) appears to be tighter than the horizontal lobe (b). B) *Phycosiphon incertum* from the viewpoint toward southeast. C) Comparison between the distribution of burrow tubes and bedding plane. D) Comparison between the bedding and flattening planes of the tubes. An oblique alignment of the flattening and bedding planes caused apparent oblique orientation of core sections of *Phycosiphon incertum*.

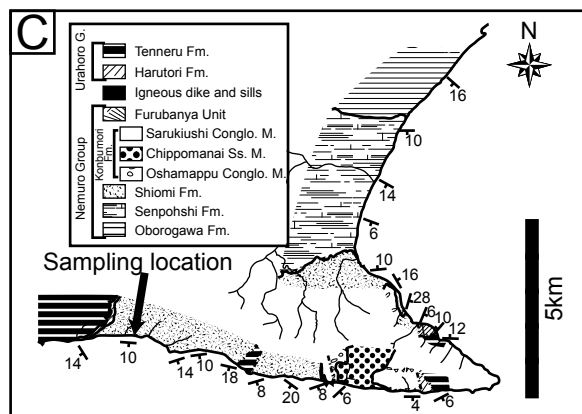
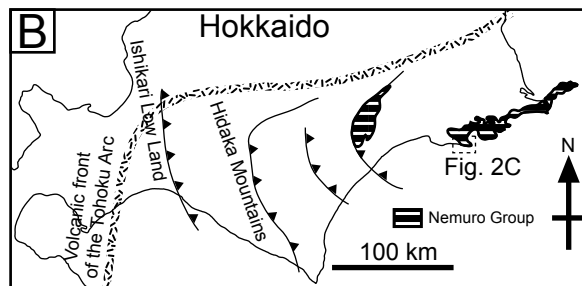
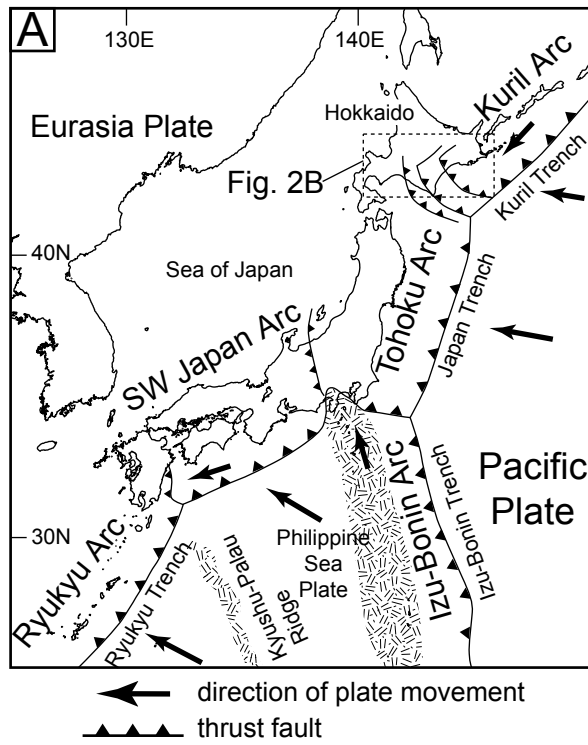
FIGURE 13—Section image of the sample along the flattening plane. Burrows perpendicular to the flattening plane have round cross section (white arrows).

FIGURE 14—Retrodeformed morphology of *Phycosiphon incertum* on the basis of flattening of burrow tubes. Curvatures of retrodeformed loops are isotropic in vertical (a) and horizontal (b) lobes, and tube thickness is relatively constant. Scale of bounding box is 8.99 mm in height, 8.73 mm width, and 6.03 mm in depth.

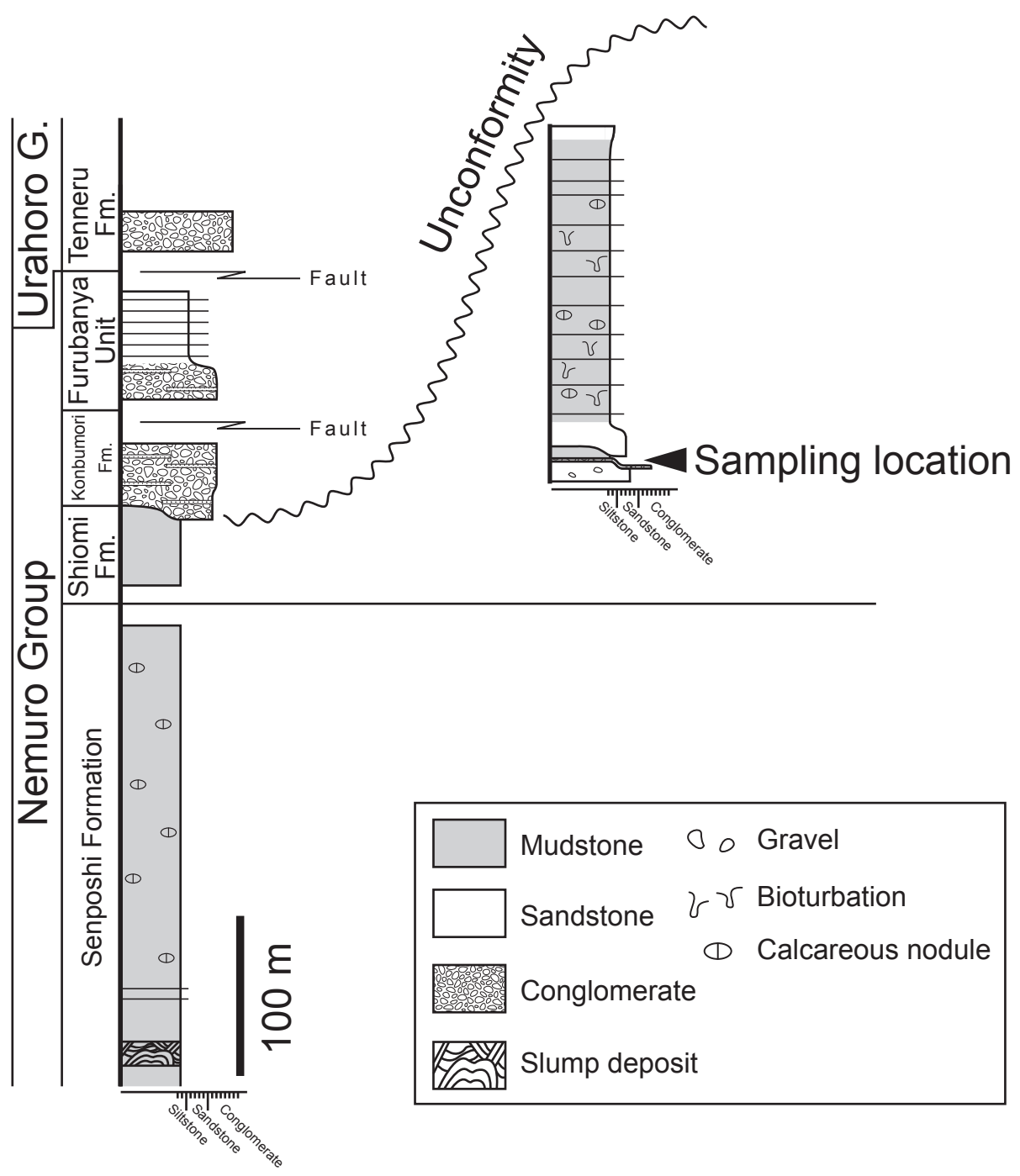
FIGURE 15—Stereonet and rose diagram indicating reconstructed slope inclination and paleocurrents of the Shiomi Formation. Tectonic tilt of bedding plane in the exterior of slump scars was corrected on the basis of flattening plane of *Phycosiphon*. Tilt-corrected inclination of submarine slope is consistent with paleocurrent direction.



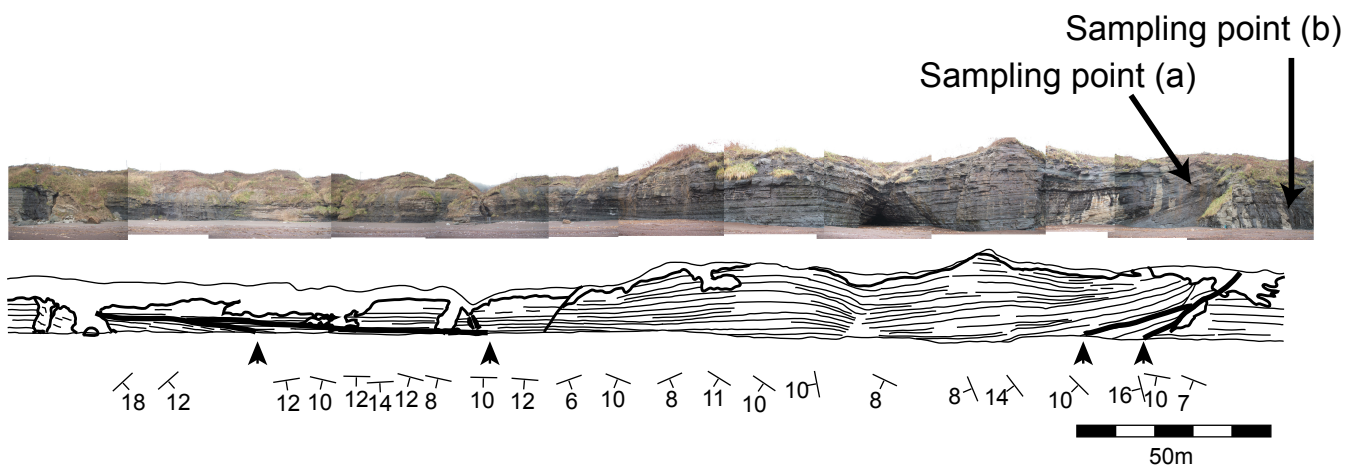
Naruse and Nifuku
Figure 1



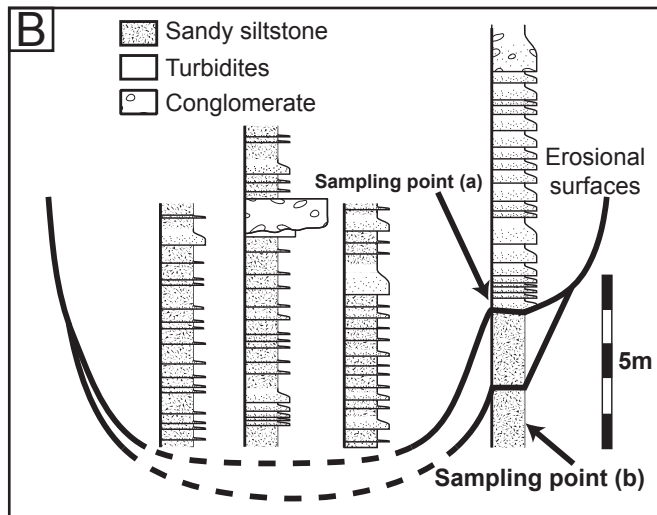
Naruse and Nifuku
Figure 2



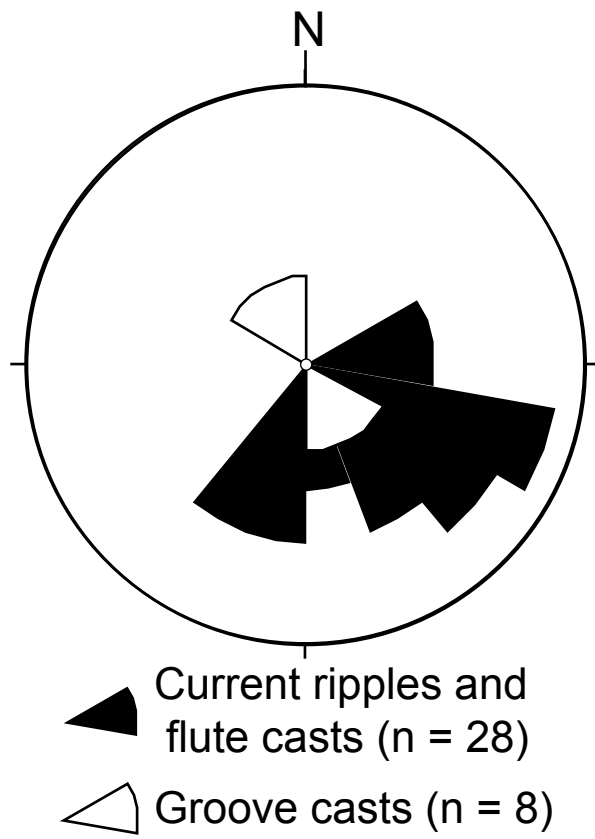
Naruse and Nifuku
Figure 3



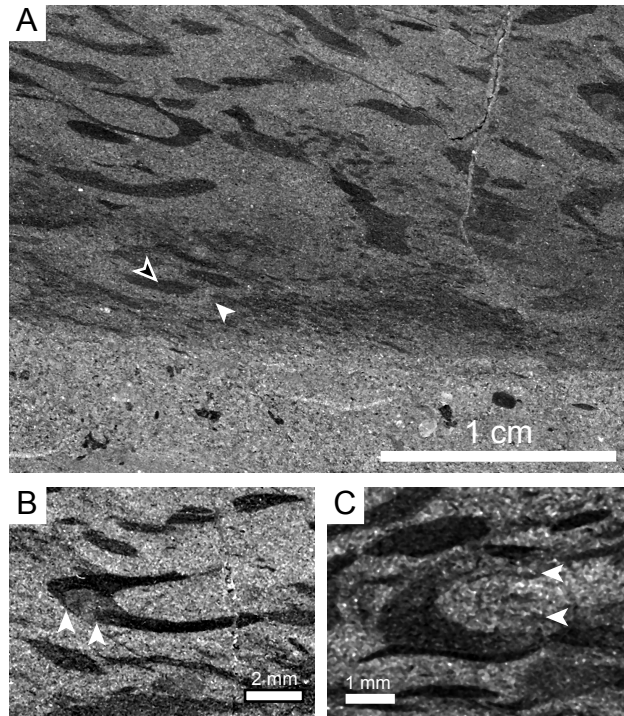
Naruse and Nifuku
Figure 4



Naruse and Nifuku
Figure 5

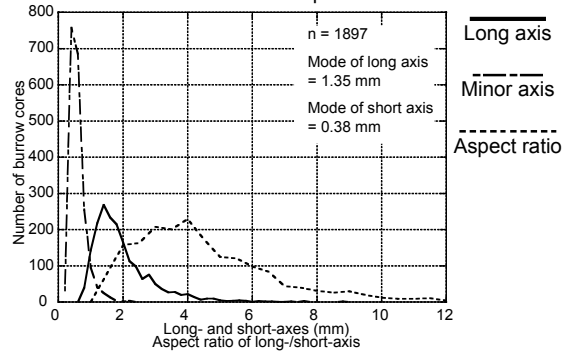


Naruse and Nifuku
Figure 6

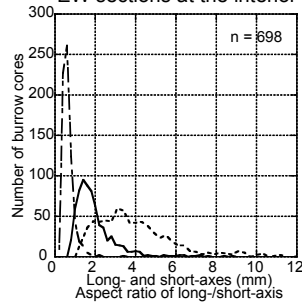


Naruse and Nifuku
Figure 7

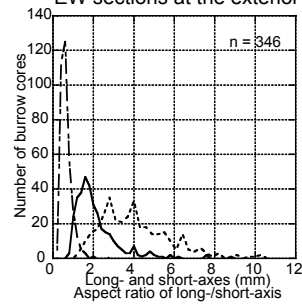
A All sections at both the interior and exterior of slump-scars



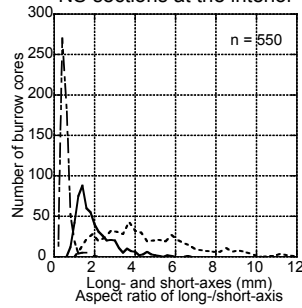
B EW sections at the interior



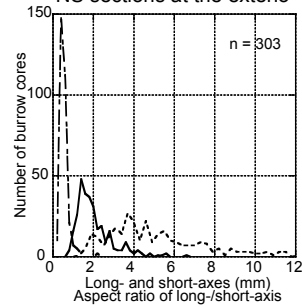
C EW sections at the exterior



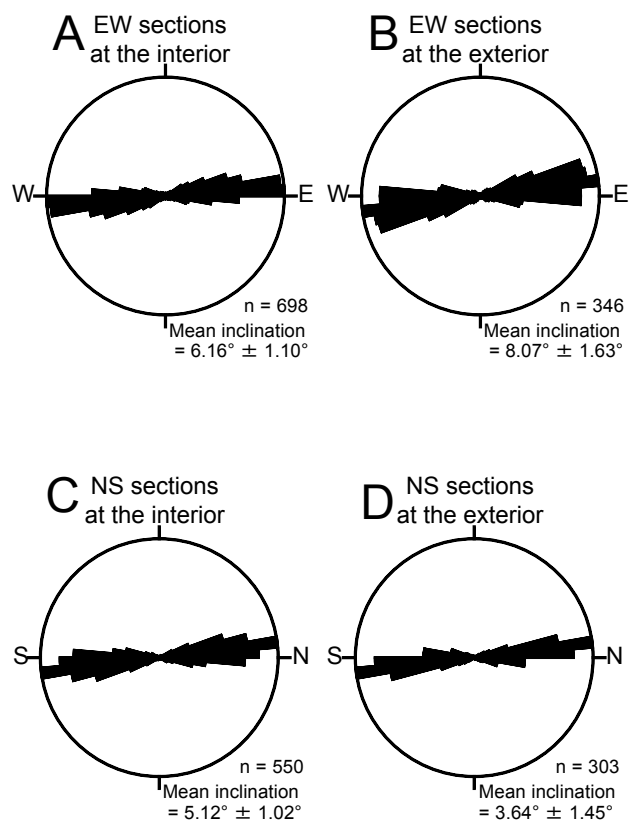
D NS sections at the interior



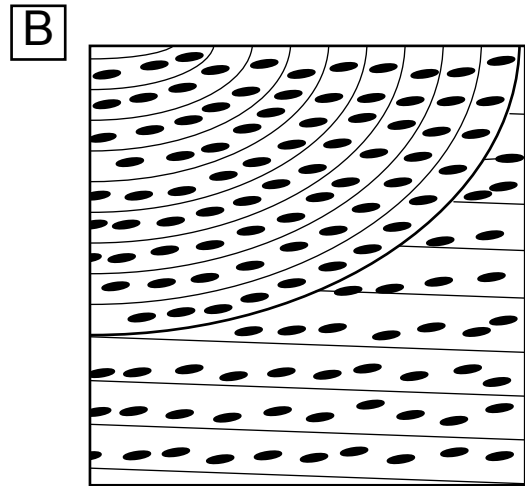
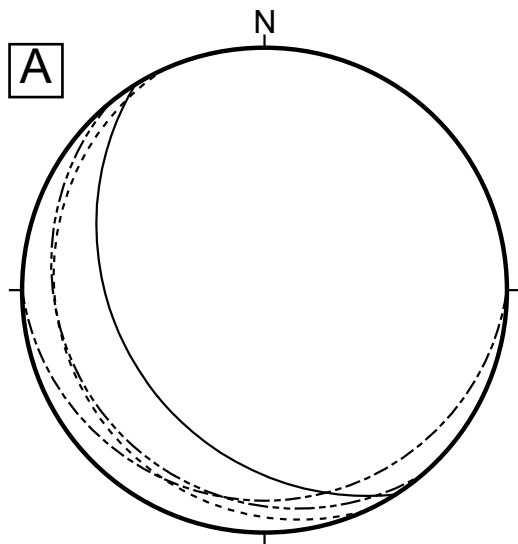
E NS sections at the exterior



Naruse and Nifuku
Figure 8



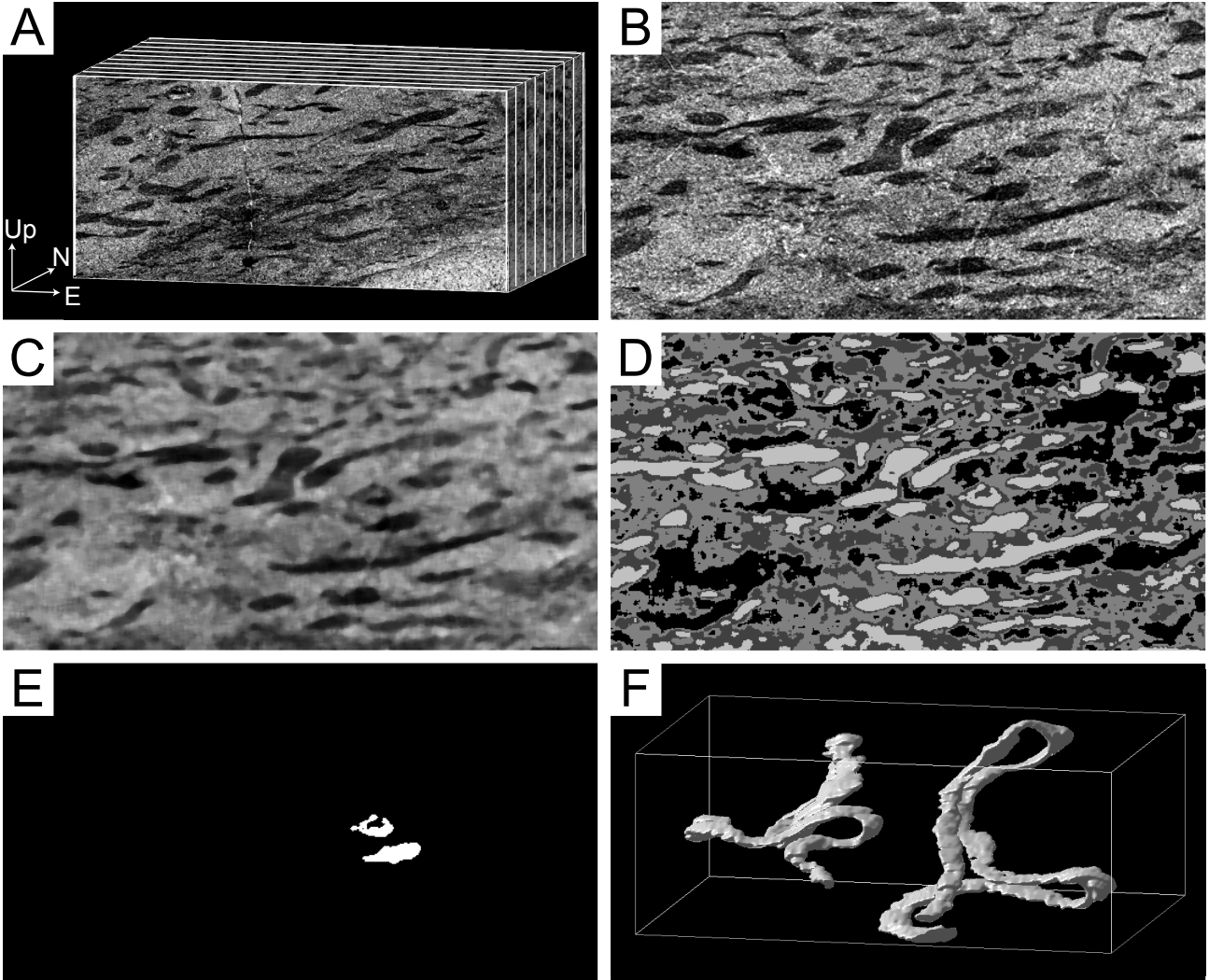
Naruse and Nifuku
 Figure 9



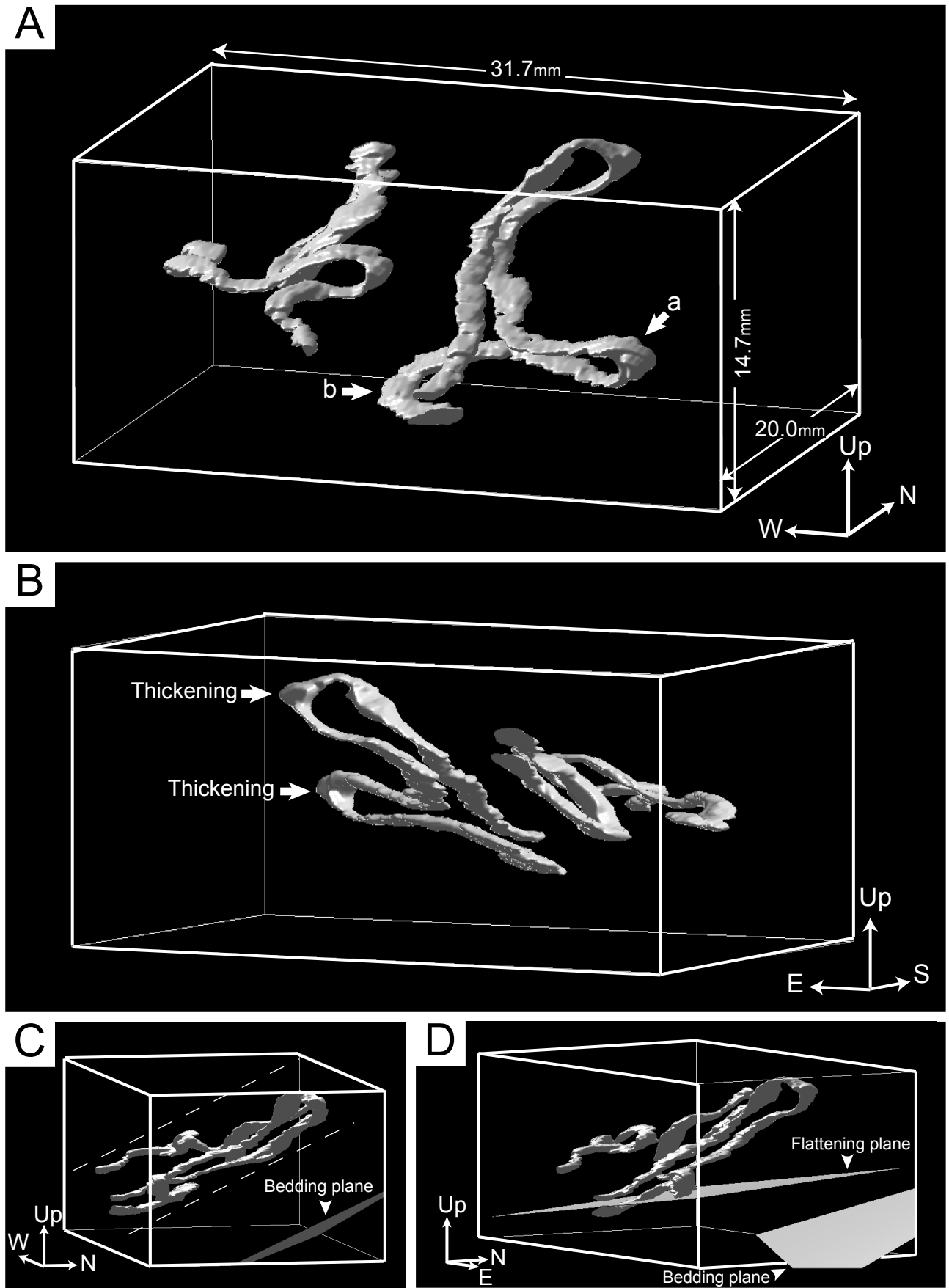
Equal angle projection, lower hemisphere

- | | | | |
|-------|---------------------------------------|-------|---------------------------------------|
| ——— | Bedding plane
in the interior | ----- | Bedding plane
in the exterior |
| ----- | <i>Phycosiphon</i>
in the interior | ----- | <i>Phycosiphon</i>
in the exterior |

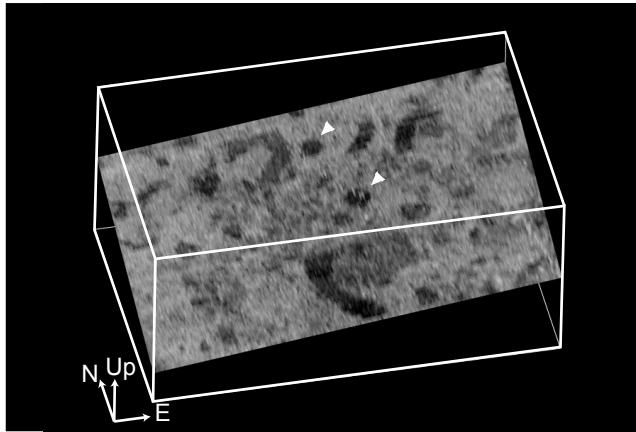
Naruse and Nifuku
Figure 10



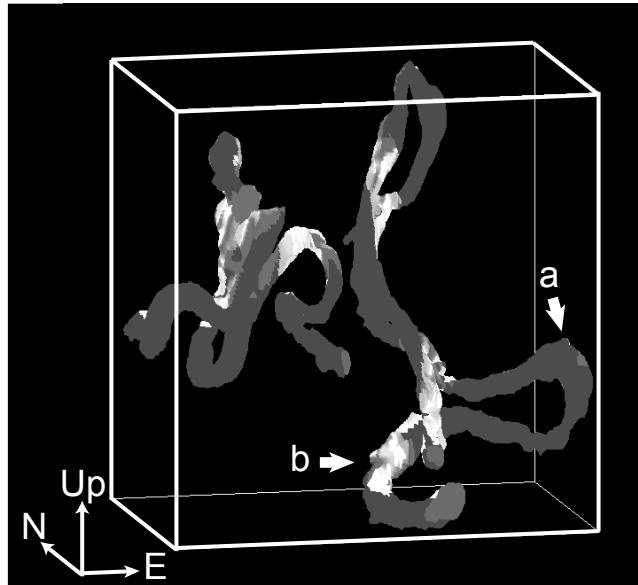
Naruse and Nifuku
Figure 11



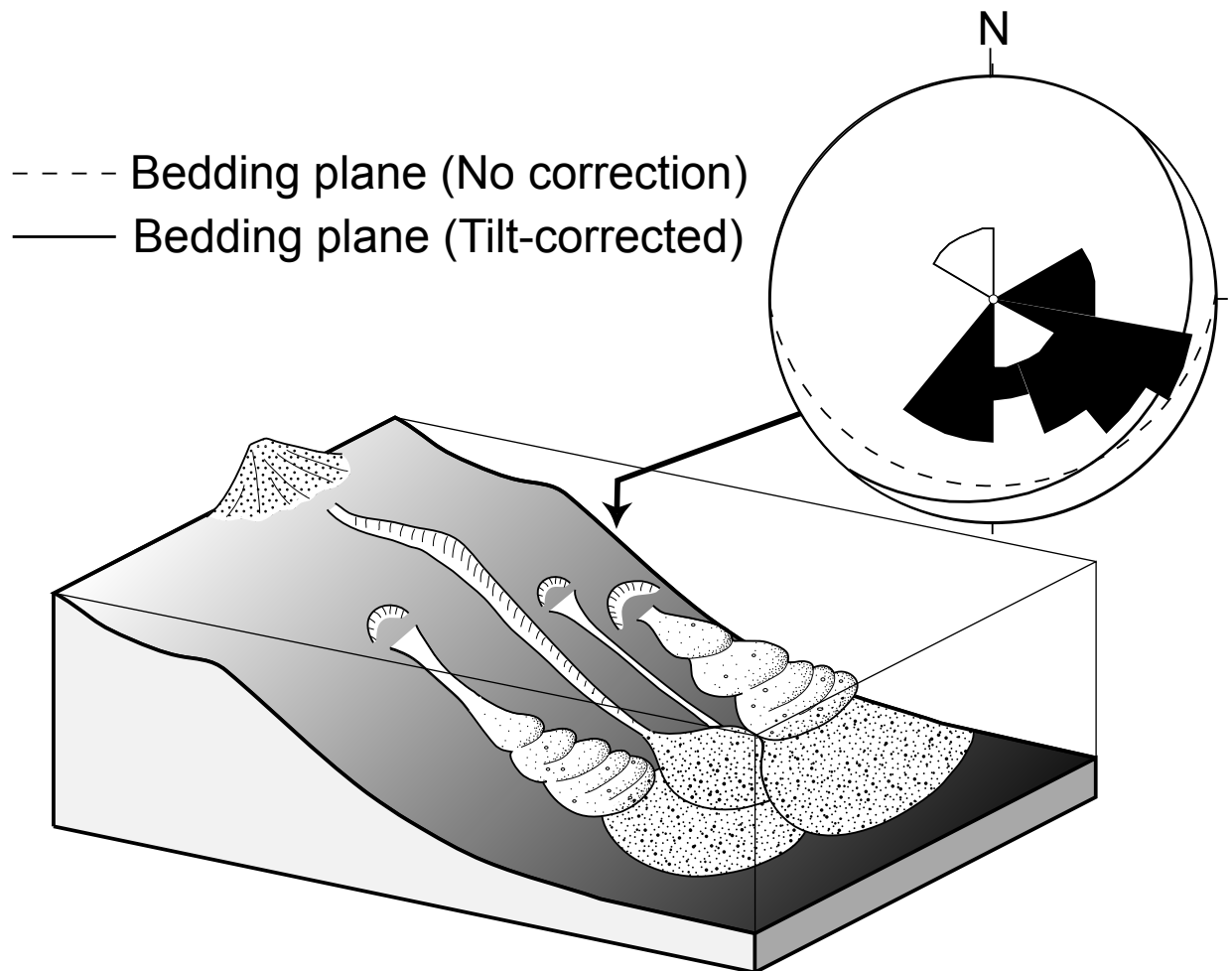
Naruse and Nifuku
Figure 12



Naruse and Nifuku
Figure 13



Naruse and Nifuku
Figure 14



Naruse and Nifuku
Figure 15